2014 SCEC Report

Proposal Number: 14033

Joint seismotectonic and source spectra analysis of the Ventura Basin and San Gorgonio Pass SCEC Special Fault Study Areas, southern California

Egill Hauksson and T.H.W. Göbel
California Institute of Technology, Seismological Laboratory, Pasadena, CA

John H. Shaw and Andreas Plesch
Harvard University, Department of Earth & Planetary Sciences, Cambridge, MA

Category:
B. Integration and Theory & C. Special Fault Study Area

Science objectives: 1a, 2d, 4d

Focus areas: EFP, SoSAFE, USR

6 March 2015

1 Summary

The slip along faults generally decreases shear stresses within earthquake source regions, however, the magnitude of the corresponding stress drops may vary widely. Variations in stress drops are thought to be a function of different crustal parameters such as heat flow, strain rate and tectonic regime. While many studies reported on systematic spatial variations in seismicity characteristics and stress drops, the primary controlling parameters of these variations remain insufficiently understood. We have analyzed the spatial variation in source parameters of small and intermediate magnitude earthquakes close to Ventura Basin and San Gorgonio Pass. In San Gorgonio, the regional tectonics are controlled by a restraining bend of the San Andreas fault system, which results in distributed crustal deformation, and heterogeneous slip along numerous strike-slip and thrust faults. Most of these faults have low geologic slip rates. Fault geometries are generally complex and much of the seismicity cannot be directly associated with specific fault surfaces. The region exhibits diffuse deformation and seismicity distributions with focal depths of up to 20 km. The Ventura region, on the other hand, is controlled by North-South compression accommodated by series of thrust and reverse faults. The Ventura region shows highly variable seismic activity that extends to depths of 20 km. The rapid convergence rates across the basin suggest that several of these faults slip at high rates and are capable of producing large-magnitude earthquakes.

We show results from a comparative study between the two regions, focusing on differences in spatial seismicity distributions, stress regimes, and stress-drops. Stress drops were estimated by fitting a Brune-type spectral model to source spectra. These spectra were obtained by an iterative stacking of the observed amplitude spectra to solve for site, path and source terms. The estimates have large scatter among individual events but the median of event populations shows systematic, statistically significant variations. We identified several crustal and faulting parameters that may contribute to local variations in stress drop including the style of faulting, changes in average tectonic slip rates, mineralogical composition of the host rocks, as well as the focal depths of seismic events. We observed anomalously-high stress drops (>20 MPa) beneath the San Gorgonio thrust faults and stress drops show an approximate negative correlation with geologic slip rates within the San Gorgonio region. The Ventura region shows significantly lower stress-drops (~1 MPa) than the San Gorgonio area. We observed a slight increase in stress-drops with depth, which can be explained, by a continuous increase in rupture velocities.

Principle stress orientations are substantially more heterogeneous within the San Gorgonio area indicating a general heterogeneity of stress accumulation and release within the area. The Ventura region shows largely homogenous principle stress orientations that are in agreement with the large-scale tectonic stresses. Stress drops are consistently low and show smaller variation compared to San Gorgonio. Our results indicate a general connection between the heterogeneity in principle stress orientations, stress drops and the spatial distribution of seismicity. Understanding underlying mechanisms of stress variations is essential to better constrain rupture propagation of major earthquakes and associated regional seismic hazards.

2 Dissemination and presentation of results

Much of the present results have been presented at key geophysics meetings (*Goebel et al.*, 2013, 2014), and were subject of a recent publication *Geophysical Journal International* (*Goebel et al.*, 2015). Another publication that includes the detailed assessment of spatial seismicity distributions and principle stress orientations is in preparation. In addition, we finished the computation of a stress drop catalog for southern California using the newly available broadband seismic record between 2000 and 2014. This stress drop catalog will be made available to the SCEC community using the usual procedures for data dissemination on the SCEC website.

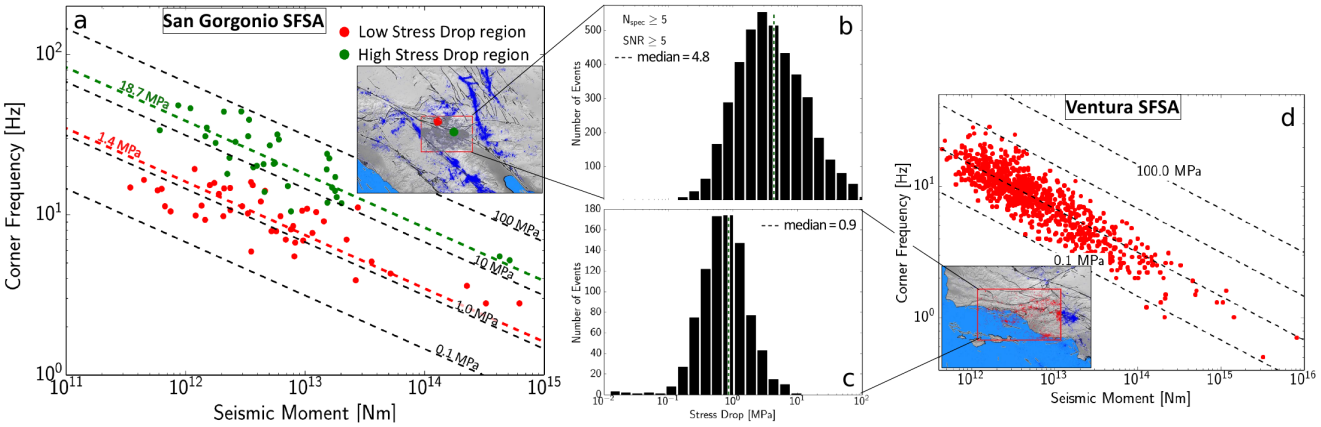

Figure 1: *Seismicity and stress drops in San Gorgonio and Ventura. San Gorgonio generally shows more distributed seismicity and larger variations in stress drops including a region of anomalously large stress drop of about 20 MPa highlighted by green dots in a). Stress drops in Ventura show less variability and seismicity occurs more localized close to the major faults within the region. In addition to smaller variability in stress drops, Ventura shows generally lower stress drops of about 1 MPa (b) & (c).*

3 Technical Report: Seismotectonics within the SCEC Special Fault Study Areas

The SCEC Special Fault Study Areas (SFSAs) are regions of complex deformation involving series of strike-slip and blind-thrust faults close to densely-populated, urban areas. Here, we analyzed seismicity, stress orientation and source parameters close to San Gorgonio Pass (SGP) and Ventura Basin (VB), which both host faults with high geometric complexity (Plesch et al., 2007). The present study is based on three different types of data: (1) A relocated earthquake catalog that improved single event location by using a 3D velocity structure, source-specific station terms and relative travel-time differences from waveform cross-correlations of event clusters (*Shearer et al.*, 2005; *Hauksson et al.*, 2012); (2) focal

mechanisms, estimated from first motion polarities and amplitude ratios of P- and S-waves (*Hardebeck and Hauksson*, 2001; *Yang et al.*, 2012); (3) seismic waveforms, obtained from the SCEC data center which we used to determine source spectra and source parameters. We limited our analysis to events that were recorded at broadband stations. These stations show a largely consistent frequency response from ~0.2–50 Hz with a sampling frequency of 100 Hz. This wide frequency band is beneficial for improving the resolution of corner frequency estimates and high-frequency fall-offs compared to previous studies. The broadband data are available for a dense array of stations in southern California starting in ~2000. We selected a period from 2000 to 2014 because of the availability of relatively homogeneous waveform records, station instrumentation and seismicity catalogs. During this period over ~ 11,300 seismic events with magnitudes in the range of M_L=0–4.88 occurred in the San Gorgonio Pass region and more than 4,000 events in the Ventura region. The largest event occurred near the San Bernardino segment of the San Andreas Fault in June 2005.

3.1 Introduction: Stress heterogeneity and possible mechanisms

Stress orientations and earthquake stress drops are influenced by local crustal conditions. For example near Parkfield, seismic off-fault events show largely self-similar scaling whereas some events on the San Andreas fault exhibit the same source pulse width, independent of event magnitudes resulting in stress drop variations between 0.18 and 63 MPa (*Harrington and Brodsky*, 2009). High stress drops for on-fault events at Parkfield were also suggested by *Nadeau and Johnson* (1998), although this result was questioned by later studies which suggested stress drop variations in Parkfield to be comparable to other areas (*Sammis and Rice*, 2001; *Allmann and Shearer*, 2007). In southern California, a comprehensive study of P-wave spectra from over 60,000 earthquakes found no correlation between stress drop and distance from major faults (*Shearer et al.*, 2006), while a study of global earthquakes with M>5 revealed higher stress drops for intraplate compared to plate boundary events (*Allmann and Shearer*, 2009). Elevated stress drops for intraplate events may be due to higher crustal strength and stresses far from active faults.

Stress drops may also be sensitive to the type of tectonic regime. For example in southern California, *Shearer et al.* (2006) identified higher-than-average stress drops in some regions containing a relatively high fraction of normal-faulting events whereas the mainly reverse-faulting aftershocks of the Northridge earthquake have lower-than-average stress drops. In contrast, the global study of *Allmann and Shearer* (2009) found higher-than-average stress drops for strike-slip events. Furthermore, stress drops are observed to be lower for regions of relatively high heat flow in Japan (*Oth*, 2013) and increase with depth, for example, in southern California (*Shearer et al.*, 2006; *Yang and Hauksson*, 2011; *Hauksson*, 2014) and Japan (*Oth*, 2013). In addition to fault proximity, tectonic regime, heat flow and depth, stress drops have also been observed to vary as a function of recurrence intervals and loading rates in the laboratory and nature (e.g. *Kanamori et al.*, 1993; *He et al.*, 2003). Slower loading rates and longer healing periods within interseismic periods lead to an increase in asperity strengths and stress drops (*Beeler et al.*, 2001).

3.2 Spectral inversion and stress drop estimates

Our method for the estimation of earthquake stress drop variations requires reliable estimates of relative differences in seismic moments and corner frequencies, which are determined in four major steps:

1. We compute P-wave amplitude spectra for each event at each station.
2. We determine relative seismic moments from local magnitudes and long-period spectral amplitudes.
3. We deconvolve the recorded event spectra into path, site and source terms.
4. We correct the source term using regional and local Empirical Green's function.
5. We determine corner frequencies by fitting the corrected source spectra with a Brune-type spectral model (*Brune*, 1970).

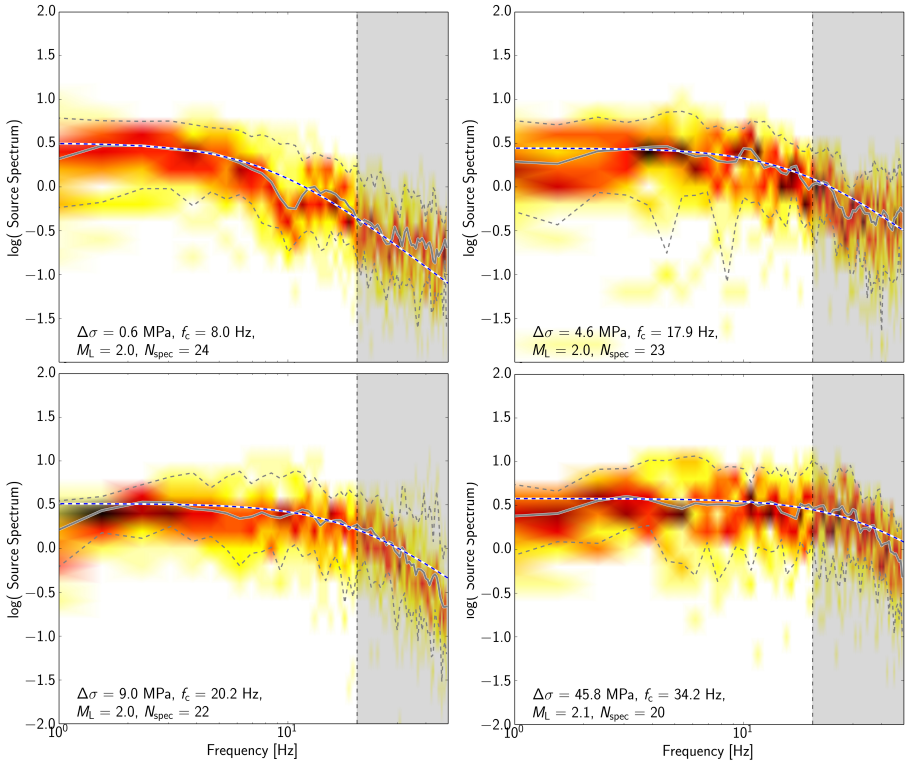

Figure 2: *Example of four events with strongly varying stress drops, i.e., similar relative moments (low frequency content) but different corner frequencies. The gray curve highlights the average source spectra for all stations and the colored areas in the background show the density of spectra from individual stations, so that warmer colors correspond to higher density of spectra. The blue dashed lines show the Brune-type spectral fits and gray, dashed curves represent the confidence bounds of the spectral density estimates as a function of frequency. The gray, shaded frequency range above 20 Hz was not included during the computation of the spectral fits.*

The recorded seismic waveforms are a convolution of site, path and source contributions. Our

source spectral inversion makes use of common ray-paths and site-effects for event clusters recorded at the same station, and common source terms for events recorded over an array of near-by stations. Source spectra are obtained by iteratively stacking the recorded amplitude spectra to isolate source, path and site terms (e.g. *Andrews*, 1986; *Warren and Shearer*, 2000; *Shearer et al.*, 2006; *Yang et al.*, 2009).

3.3 Stress drop heterogeneity within the greater San Gorgonio Pass region

The SGP region has received much attention because of its likely role in hindering or supporting a large-magnitude, through-going earthquake rupture on the southern San Andreas (e.g. *Magistrale and Sanders*, 1996; *Graves et al.*, 2008). This region also provides an ideal natural-laboratory to study stress drop variations because of its high seismic activity, station density and well-studied tectonics. One of the fundamental questions concerning the SGP region is the possibility of large ruptures that could propagate through the entire region, e.g., from Cajon Pass to the Salton Sea (*Graves et al.*, 2008). Using the average fault orientation within the Mojave segment, we determined variations in stress drop estimates in the proximity of a possible path of such a rupture between the San Bernardino and Garnet Hill segment (Figure 3). The stress drops decrease to the southeast of SGP within the area of the Banning and Garnet Hill segments, which eventually merge with the Coachella segment of the San Andreas Fault. The stress drops also decrease to the northwest of SGP and show consistently lower values outside of the SGF segment.

The stress drop traverse through the SGP is located in immediate proximity to local slip rate estimates along the SAF. Geologic slip rates were previously compiled from many different studies and summarized by *Dair and Cooke* (2009); *Cooke and Dair* (2011) as well as by *McGill et al.* (2013) highlighting a systematic decrease from Cajon Creek (slip rates = 24.5 ± 3.5 mm/yr) to Cabezon (5.7 ± 0.8 mm/yr), which is close to SGP. To the southeast, the slip rates increase again within the Coachella region (14–17 mm/yr) of the San Andreas Fault. The average geologic slip rate on the SGF itself is estimated to be as low as 1.0–1.3 mm/yr (*Matti et al.*, 1992). Stress drop estimates show a statistically significant increase from ~3–10 MPa before decreasing again southeast of SGP. This shows that stress drop and slip rate estimates are approximately inversely correlated along the profile of the San Andreas Fault zone. The stress drop estimates are, in contrast to slip rate estimates, based on small-magnitude events that occur off the major fault segments. This may imply that low slip rate estimates, e.g. for the SGP, are representative for the numerous adjacent, secondary-faults that are discussed in more detail below (see also *Goebel et al.*, 2015, for more details).

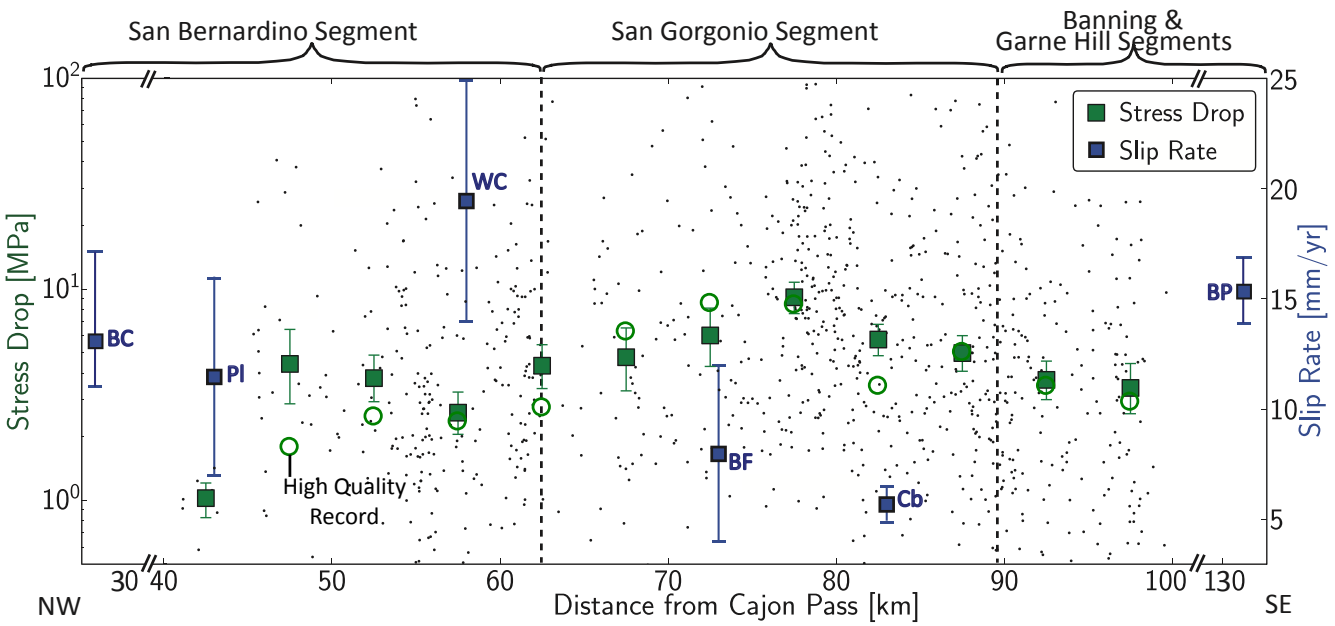

Figure 3: *Changes in stress drop across the SGP region, i.e. within a ~ 10 km wide area around the San Andreas fault zone from NW to SE. The x-axis displays the distance along the San Andreas from Cajon pass. Individual event stress drops are marked by gray dots and distance-binned, mean values by green squares. The 95% confidence bounds of the mean, estimated by bootstrap resampling, are highlighted by green error bars. Geologic slip rates and uncertainties along the transect are highlighted by blue squares and blue error bars. The variation in mean stress drops with slip rates, e.g., between Pl ($\Delta\sigma = 1 - 3$ MPa) and BF ($\Delta\sigma = 7 - 8$ MPa) is statically significant at the 99% level. Sites of geologic slip rate estimates: BC: Badger Canon (McGill et al., 2013), Pl: Plunge Creek (McGill et al., 2013), WC: Wilson Creek (Weldon and Sieh, 1985), BF: Burro flats (Orozco and Yule, 2003), Cb: Cabezon (Yule et al., 2001), BP: Biskra Palms (Behr et al., 2010). Stress drop results for the high quality dataset (open circles).*

3.4 Seismic velocities and stress heterogeneity in the Ventura and San Gorgonio regions

In addition, to the detailed analysis of stress drop variations, we investigated seismicity distributions and seismic velocities within the two study areas. Both regions are characterized by earthquakes with large focal depth extending down to 20 km or more. The SGP region is substantially more active seismically showing widely distributed earthquakes. These seismic events can only partially be connected to the location of known fault surfaces and much of the seismicity occurs off the major faults. Ventura Basin is characterized by lower seismic velocities associated with the deep (locally > 10km) sedimentary basin (Shaw et al., 2015), which hosts only limited seismic activity.

One of the most striking difference between the two regions is the large variability in principle stress orientations in SGP and lack thereof in VB. Assuming that the P-axes are a proxy for the average direction and overall variability in the principle stress orientations, we compare the

stress field in VB and SGP. The VB region shows a locally more homogeneous stress field that is roughly in agreement with NNE-SSW compression. SGP, on the other hand, shows more variability in P-axes and principle stress orientations: an expression of more small-scale heterogeneity likely originating from the geometric complexity of the San Andreas fault system with the study area, which includes strike-slip, thrust, and reverse faults or varying orientations (Plesch et al., 2007).

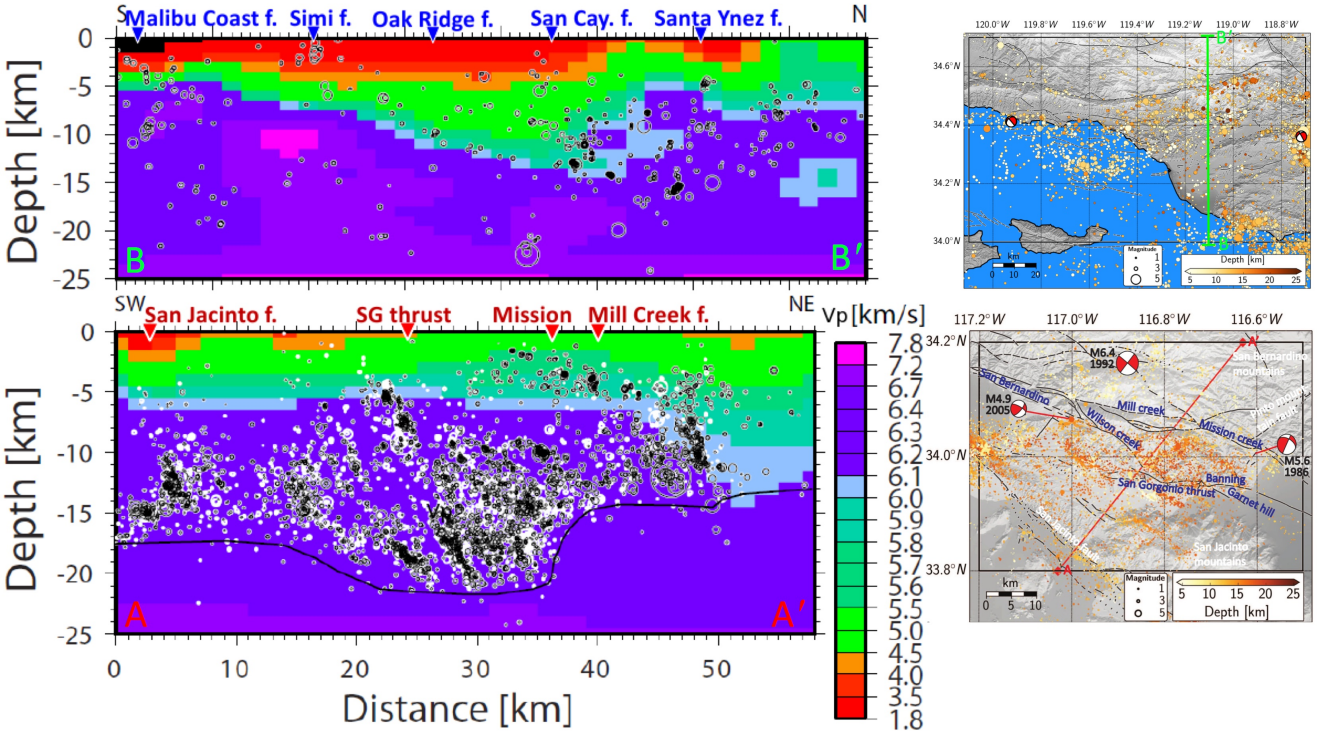

Figure 4: *P-wave velocity model (CVM-H) for VB and SGP. VB shows an area of lower V_p-values within and a relatively abrupt increase north of the basin where the focal depths extend down to about 20 km. The SGP area shows generally little lateral variations in V_p and seismic velocities increase more gradually with depth.*

3.5 Conclusion

We have analyzed the spatial variation in stress orientations and source parameters of small and intermediate magnitude earthquakes within the San Gorgonio Pass and Ventura regions. Our analysis revealed earthquakes with relatively high stress drops (>20 MPa) between the surface traces of the San Gorgonio thrust and Mission fault. The Ventura region showed little variation in stress drops and average stress drops are low (~1 MPa). Stress drop estimates in San Gorgonio are approximately inversely correlated with long-term slip rates along the San Andreas Fault system so that rapidly loaded fault zones are connected to lower stress drops whereas slow-slipping faults create events with higher stress drops. Our study revealed

generally large heterogeneity in stresses in San Gorgonio expressed by large variability in stress drops and stress orientations. Ventura, on the other hand, is characterized by consistently low stress drops and little heterogeneity in principle stress orientations. A better documentation of stress heterogeneity in Southern California is essential to constrain rupture propagation of major earthquakes and associated regional seismic hazards.

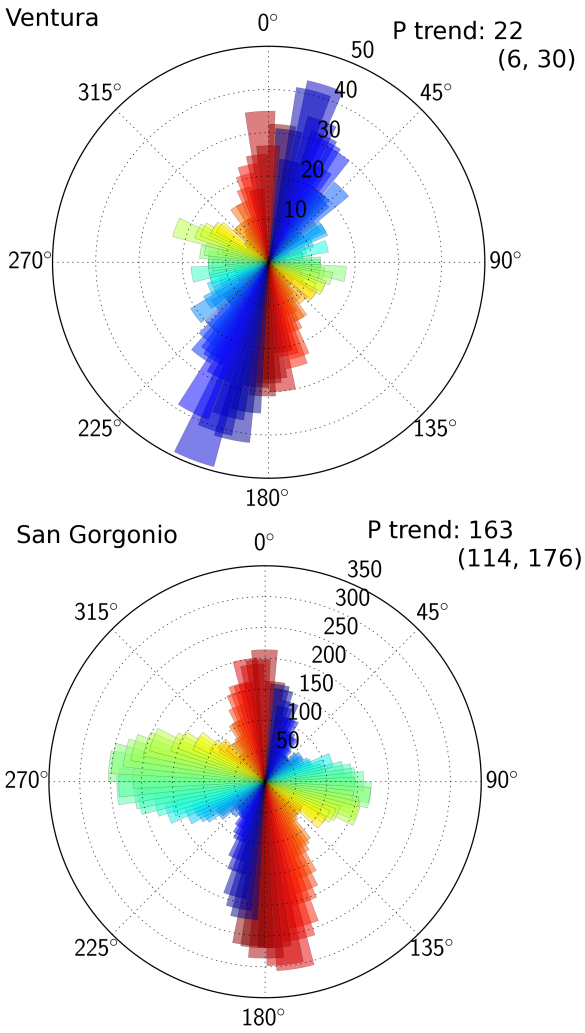

Figure 5: *P-axes orientations in VB (top) and SGP (bottom). Median values and confidence interval are given in the upper right corner of each subplot.*

References

Allmann, B. P., and P. M. Shearer (2007), Spatial and temporal stress drop variations in small earthquakes near Parkfield, California, *J. Geophs. Res.*, *112*(B4), B04,305.

Allmann, B. P., and P. M. Shearer (2009), Global variations of stress drop for moderate to

large earthquakes, *J. Geophys. Res.*, *114*(B1), B01,310.

Andrews, D. J. (1986), Objective determination of source parameters and similarity of earthquakes of different size, *in Earthquake Source Mechanics*, pp. 259–267, doi:10.1029/GM037p0259.

Beeler, N. M., S. H. Hickman, and T.-f. Wong (2001), Earthquake stress drop and laboratory-inferred interseismic strength recovery, *J. Geophys. Res.*, *106*(B12), 30,701–30,713.

Behr, W., et al. (2010), Uncertainties in slip-rate estimates for the Mission Creek strand of the southern San Andreas fault at Biskra Palms Oasis, Southern California, *Geo. Soc. Am. Bull.*, *122*, 1360–1377, doi: 10.1130/B30020.1.

Brune, J. N. (1970), Tectonic stress and the spectra of seismic shear waves from earthquakes, *J. Geophys. Res.*, *75*(26), 4997–5009.

Cooke, M. L., and L. C. Dair (2011), Simulating the recent evolution of the southern big bend of the San Andreas fault, Southern California, *J. Geophys. Res.*, *116*(B4).

Dair, L., and M. L. Cooke (2009), San Andreas fault geometry through the San Gorgonio Pass, California, *Geology*, *37*(2), 119–122.

Goebel, T. H. W., E. Hauksson, J.-P. Ampuero, and P. M. Shearer (2013), Stress drop heterogeneity within the southern california plate boundary fault system, *AGU 2013 Annual Meeting, San Fransisco, Abstracts*.

Goebel, T. H. W., E. Hauksson, A. Plesch, and J. Shaw (2014), A comparative study of Seismotectonics in the San Gorgonion and Ventura Special Fault Study Areas, *Southern California Earthquake Center Annual Meeting, Proceedings and Abstracts*, *24*.

Goebel, T. H. W., E. Hauksson, J.-P. Ampuero, and P. M. Shearer (2015), Stress drop heterogeneity within tectonically complex regions: A case study of San Gorgonio pass, Southern California, *Geophys. J. Int.*, doi:GJI-S-14-0861, (in revision).

Graves, R. W., B. T. Aagaard, K. W. Hudnut, L. M. Star, J. P. Stewart, and T. H. Jordan (2008), Broadband simulations for M_W 7.8 southern San Andreas earthquakes: Ground motion sensitivity to rupture speed, *Geophys. Res. Lett.*, *35*(22).

Hardebeck, J. L., and E. Hauksson (2001), Stress orientations obtained from earthquake focal mechanisms: What are appropriate uncertainty estimates?, *Bull. Seismol. Soc. Am.*, *91*, 250–262, doi: 10.1785/0120000032.

Harrington, R. M., and E. E. Brodsky (2009), Source duration scales with magnitude differently for earthquakes on the San Andreas Fault and on secondary faults in Parkfield, California, *Bull. Seismol. Soc. Am.*, *99*(4), 2323–2334.

Hauksson, E. (2014), Average stress drops of southern California earthquakes in the context of crustal geophysics: Implications for fault zone healing, *Pure Appl. Geophys.*, pp. 1–12, doi:10.1007/s00024-014- 0934-4.

Hauksson, E., W. Yang, and P. M. Shearer (2012), Waveform relocated earthquake catalog for Southern California (1981 to june 2011), *Bull. Seism. Soc. Am.*, *102*(5), 2239–2244.

He, C., T.-f. Wong, and N. M. Beeler (2003), Scaling of stress drop with recurrence interval and loading velocity for laboratory-derived fault strength relations, *J. Geophys. Res.*, *108*(B1), doi: 10.1029/2002JB001890.

Kanamori, H., J. Mori, E. Hauksson, T. H. Heaton, L. K. Hutton, and L. M. Jones (1993), Determination of earthquake energy release and m_l using terrascope, *Bull. Seismol. Soc. Am.*, *83*(2), 330–346.

Magistrale, H., and C. Sanders (1996), Evidence from precise earthquake hypocenters for segmentation of the San Andreas fault in San Gorgonio Pass, *J. Geophys. Res.*, *101*(B2), 3031–3044.

Matti, J., D. Morton, and B. Cox (1992), The San Andreas fault system in the vicinity of the central Transverse Ranges province, Southern California, *U.S. Geol. Surv., Reston, Va.*, *40*, 92–354.

McGill, S. F., L. A. Owen, R. J. Weldon, and K. J. Kendrick (2013), Latest Pleistocene and Holocene slip rate for the San Bernardino strand of the San Andreas fault, Plunge Creek, Southern California: Implications for strain partitioning within the southern San Andreas fault system for the last ~ 35 ky, *Geol. Soc. Am. Bull.*, *125*(1-2), 48–72.

Nadeau, R. M., and L. R. Johnson (1998), Seismological studies at parkfield VI: Moment release rates and estimates of source parameters for small repeating earthquakes, *Bull. Seismol. Soc. Am.*, *88*(3), 790–814.

Orozco, A., and D. Yule (2003), Late Holocene slip rate for the San Bernardino strand of the San Andreas Fault near Banning, California, *Seis. Res. Lett.*, *74*(2), 237.

Oth, A. (2013), On the characteristics of earthquake stress release variations in Japan, *Earth and Planetary Science Letters*, *377*, 132–141.

Plesch, A., and J. H. Shaw, C. Benson, W.A. Bryant, S. Carena, M. Cooke, J. F. Dolan, G. Fuis, E. Gath, L. Grant, E. Hauksson, T. H. Jordan, M. Kamerling, M. Legg, S. Lindvall, H. Magistrale, C. Nicholson, N. Niemi, M. E. Oskin, S. Perry, G. Planansky, T. Rockwell, P. Shearer, C. Sorlien, M. P. Suess, J. Suppe, J. Treiman, and R. Yeats (2007), Community Fault Model (CFM) for Southern California, *Bulletin of the Seismological Society of America*, Vol. 97, No. 6, p. 1793–1802.

Sammis, C. G., and J. R. Rice (2001), Repeating earthquakes as low-stress-drop events at a

border between locked and creeping fault patches, *Bull. Seismol. Soc. Am.*, *91*(3), 532–537.

Shaw, J. H., A. Plesch, C. Tape, M. P. Suess, T. H. Jordan, G. Ely, E. Hauksson, J. Tromp, T. Tanimoto, R. Graves, K. Olsen, C. Nicholson, P. J. Maechling, C. Rivero, P. Lovely, C. M. Brankman, J. Munster (2015), Unified Structural Representation of the southern California crust and upper mantle, *Earth and Planetary Science Letters,* 415, 1–15.

Shearer, P., E. Hauksson, and G. Lin (2005), Southern California hypocenter relocation with waveform cross-correlation, part 2: Results using source-specific station terms and cluster analysis, *Bull. Seismol. Soc. Am.*, *95*(3), 904–915.

Shearer, P. M., G. A. Prieto, and E. Hauksson (2006), Comprehensive analysis of earthquake source spectra in southern California, *J. Geophs. Res.*, *111*(B6), B06,303.

Warren, L. M., and P. M. Shearer (2000), Investigating the frequency dependence of mantle Q by stacking P and PP spectra, *J. Geophys. Res.*, *105*(B11), 25,391–25.

Weldon, R. J., and K. E. Sieh (1985), Holocene rate of slip and tentative recurrence interval for large earthquakes on the San Andreas fault, Cajon Pass, southern California, *Geol. Soc. Am. Bull.*, *96*(6), 793– 812.

Yang, W., and E. Hauksson (2011), Evidence for vertical partitioning of strike-slip and compressional tectonics from seismicity, focal mechanisms, and stress drops in the east Los Angeles basin area, California, *Bull. Seismol. Soc. Am.*, *101*(3), 964–974.

Yang, W., Z. Peng, and Y. Ben-Zion (2009), Variations of strain-drops of aftershocks of the 1999 I ̇zmit and Düzce earthquakes around the Karadere-Düzce branch of the North Anatolian Fault, *Geophys. J. Int.*, *177*(1), 235–246.

Yang, W., E. Hauksson, and P. M. Shearer (2012), Computing a large refined catalog of focal mechanisms for southern California (1981–2010): Temporal stability of the style of faulting, *Bull. Seismol. Soc. Am.*, *102*(3), 1179–1194.

Yule, D., T. Fumal, S. McGill, and G. Seitz (2001), Active tectonics and paleoseismic record of the San Andreas fault, Wrightwood to Indio: Working toward a forecast for the next ’Big Event’, *Geologic Excursions in the California Deserts and Adjacent Transverse Ranges*, pp. 91–126.